Dynamic mean-field theory and the like

Jinyuan Wu

December 20, 2022

1 Introduction

Suppose we are to find the single-particle Green function of a condensed matter system. The standard procedure is to find the irreducible self-energy Σ by Feynman diagram resummation (although there are subtleties concerning the well-definedness and uniqueness of Feynman diagram resummation techniques [1, 2]). In strongly correlated systems, deciding diagrams with most contributions is generally hard, and brutal-force resummation proves intractable.

If, however, it is found that the self-energy (or two-particle vertex, or similar "n-particle self-energy diagrams") is highly local, then in principle, it can be replicated in a *few-body* model, although as we are going to see below, it is just formally few-body: its most natural form is better described as a *many-body impurity model*. Suppose, for example, that the real space self-energy $\Sigma_{\boldsymbol{ij}}$ is only important when $|\boldsymbol{i}-\boldsymbol{j}| \leq n$. Then we can just choose a cluster of sites satisfying the $|\boldsymbol{i}-\boldsymbol{j}| \leq n$ condition, and integrate out the rest of electron modes, and in the resulting impurity model, $\Sigma_{\boldsymbol{ij}}$ is exactly the same as in the original model. The main obstacle now is to decide the parameters in this new impurity model, which can be solved by adopting a self-consistent scheme: $\Sigma_{\boldsymbol{ij}}$, together with the free part of the original model, decides the one-particle Green function, which then can be used to fit the parameters in the impurity model, and then the impurity model can be solved to update the self-energy.

It can be seen that diagrammatically speaking, this idea is also a resummation strategy, though here we pick up diagrams according to their *locality* instead of structures, and the local parts of *all* diagrams, as long as they fit in the ansatz of the impurity model, are included when we solve the impurity model. This can also be seen as a mean-field approach, just like other self-consistent Feynman diagram resummation strategies. Since the parameters in the impurity model may contain time explicitly, we may say what we are doing is a *dynamic* mean-field theory.

This report reviews the development of dynamic mean-field theory (DMFT). The term *dynamic mean-field theory* is usually reserved for the most coarse approximation with a single-site cluster and a completely space-independent self-energy discussed in Section 2. In Section 3, we move beyond the simplest DMFT scheme and increase the number of sites and loose the locality requirement for the self-energy. Section 4 is about combining DMFT and *ab initio* methods together.

2 DMFT for the Hubbard model

2.1 Duality between the Hubbard model and the Anderson impurity model

In this section we discuss DMFT for the Hubbard model

$$H = -t \sum_{\langle \boldsymbol{i},\boldsymbol{j}\rangle,\sigma} c^\dagger_{\boldsymbol{i}\sigma} c_{\boldsymbol{j}\sigma} + \text{h.c.} + U \sum_{\boldsymbol{i}} n_{\boldsymbol{i}\uparrow} n_{\boldsymbol{j}\downarrow} - \mu N. \tag{1}$$

The free part results in the imaginary time Green function

$$G_0(\mathrm{i}\omega_n, \boldsymbol{k}\sigma) = G_0(\mathrm{i}\omega_n, \boldsymbol{k}), \quad G_0(\mathrm{i}\omega_n, \boldsymbol{k}) = \frac{1}{\mathrm{i}\omega_n - \varepsilon_{\boldsymbol{k}} + \mu}, \tag{2}$$

where $\varepsilon_{\boldsymbol{k}}$ is the band structure of the tight-binding model part. Now we map the Hubbard model to an impurity theory. We keep only one site in the impurity theory and integrate out the rest, and the final effective theory looks like

$$S_{\text{single site}} = -\int \mathrm{d}\tau \int \mathrm{d}\tau'\, \bar{c}(\tau)\mathcal{G}^{-1}(\tau-\tau')c(\tau') + \int \mathrm{d}\tau\, U n_\uparrow(\tau) n_\downarrow(\tau). \tag{3}$$

The Green function $\mathcal{G}(\tau)$ is $G_{0,\boldsymbol{ii}}(\tau)$ corrected by the integrated out electronic degrees of freedom; the local interaction $Un_\uparrow n_\downarrow$ is not included in $\mathcal{G}$.

Note that $\mathcal{G}$ can also be seen as a single-particle Green function with self-energy correction, and therefore has the same structure of a self-energy-corrected single-particle Green function, although its value is different from $G_{\boldsymbol{ii}}$, because its self-energy is different from the self-energy of the whole Hubbard system, since the former only considers sites beside $\boldsymbol{i}$ while the latter considers all sites. Assuming the self-energy of $\mathcal{G}$ is well-behaved for Hilbert transformation [3], we write the structure of $\mathcal{G}$ as

$$\mathcal{G}(\mathrm{i}\omega_n)^{-1} = \mathrm{i}\omega_n + \text{const.} + \int \mathrm{d}\epsilon\, g(\epsilon) \frac{1}{\mathrm{i}\omega_n - \epsilon},$$

and this means the single-site model can be instantiated by replacing $\mathcal{G}$ by a bath of non-interactive electrons, the dispersion relations of which are decided by poles of $\mathcal{G}$, and we get an Anderson impurity model

$$H_{\text{Anderson}} = \underbrace{\epsilon_0 \sum_\sigma c_\sigma^\dagger c_\sigma + \sum_{\boldsymbol{k},\sigma} E_{\boldsymbol{k}} d_{\boldsymbol{k}\sigma}^\dagger d_{\boldsymbol{k}\sigma} + \sum_{\boldsymbol{k}} (V_{\boldsymbol{k}} d_{\boldsymbol{k}\sigma}^\dagger c_\sigma + \text{h.c.})}_{\simeq c^\dagger \mathcal{G} c} + Un_\uparrow n_\downarrow. \tag{4}$$

The structure of $\mathcal{G}$ is therefore

$$\mathcal{G}(\mathrm{i}\omega_n) = \frac{1}{\mathrm{i}\omega_n - \epsilon_0 - \Delta(\mathrm{i}\omega_n)}, \quad \Delta(\mathrm{i}\omega_n) = \sum_{\boldsymbol{k}} \frac{|V_{\boldsymbol{k}}|^2}{\mathrm{i}\omega_n - E_{\boldsymbol{k}}}. \tag{5}$$

Note that the influence of $Un_\uparrow n_\downarrow$ is not accounted for by $\mathcal{G}$. Other Hamiltonian realizations of (3) are of course possible [3]. Note that here Δ contains explicitly $\mathrm{i}\omega_n$ and therefore has retardation effects in the real space. Therefore (3) contains retardation, and this is an evidence why it is better to put it into the form of a *many-body* impurity model instead of a single-body model.

We use G_{imp} to refer to the interaction-corrected Green function in the impurity model. Note that by definition of the mapping, we have $G_{\text{imp}}(\mathrm{i}\omega_n) = G_{\boldsymbol{ii}}(\mathrm{i}\omega_n)$, and therefore

$$\frac{1}{\mathcal{G}(\mathrm{i}\omega_n)^{-1} - \Sigma_{\text{imp}}} = G_{\text{imp}}(\mathrm{i}\omega_n) = G_{\boldsymbol{ii}}(\mathrm{i}\omega_n) = \frac{1}{N}\sum_{\boldsymbol{k}} G(\mathrm{i}\omega_n, \boldsymbol{k}) = \frac{1}{N}\sum_{\boldsymbol{k}} \frac{1}{\mathrm{i}\omega_n - \epsilon_{\boldsymbol{k}} - \Sigma(\mathrm{i}\omega_n, \boldsymbol{k})}. \tag{6}$$

where G is the fully corrected Green function in the Hubbard model, Σ is the self-energy of the Hubbard model, and Σ_{imp} is the self-energy correction to $\mathcal{G}$ caused by $Un_\uparrow n_\downarrow$.

2.2 The self-energy locality condition

The mapping from a Hubbard model to an Anderson impurity model involves no physical approximation. Now we impose the locality condition of the self-energy mentioned in the introduction: we assume the Hubbard model self-energy $\Sigma(\mathrm{i}\omega_n, \boldsymbol{k})$ is highly localized in the real space, and therefore involves no $\boldsymbol{k}$-dependence, and thus we immediately get

$$\Sigma_{\text{imp}} = \Sigma(\mathrm{i}\omega_n \boldsymbol{k}). \tag{7}$$

This approximation is exact in an infinite lattice [4], and therefore expectedly works better for bulk materials than monolayer materials.

2.3 The self-consistent loop

The cutoff (7) gives us a self-consistent calculation scheme: first using G_0 (known) and Σ_{imp} (from last iteration), we have

$$G(\mathrm{i}\omega_n, \boldsymbol{k}) = \frac{1}{\mathrm{i}\omega_n - \varepsilon_{\boldsymbol{k}} + \mu - \Sigma_{\text{imp}}(\mathrm{i}\omega_n)}, \tag{8}$$

and then we calculate $G_{\boldsymbol{ii}}$ (essentially G_{imp}) by

$$G_{\boldsymbol{ii}}(\mathrm{i}\omega_n) = \frac{1}{N}\sum_{\boldsymbol{k}} G(\mathrm{i}\omega_n, \boldsymbol{k}), \tag{9}$$

and then $\mathcal{G}$ can be found by

$$\mathcal{G}(\mathrm{i}\omega_n)^{-1} = G_{\boldsymbol{ii}}(\mathrm{i}\omega_n)^{-1} + \Sigma_{\mathrm{imp}}(\mathrm{i}\omega_n). \tag{10}$$

Now the impurity model is fully determined, and with U and $\mathcal{G}(\mathrm{i}\omega_n)$, we solve the model and get G_{imp}. So now G_{imp} is updated, and we can then find the updated Σ_{imp}, and we go back to the starting point of the loop.

Note that here Σ_{imp} is *not* calculated using diagrammatic resummation techniques. Instead, we find G_{imp} without explicitly mentioning Σ_{imp} in the impurity solver step, and Σ_{imp} is found *after* G_{imp} (and $\mathcal{G}$) is known. This guarantees enough accuracy of Σ_{imp}: if it is evaluated in the same way with, say, the GW method, infinite diagrams are thrown away, but here *all* Feynman diagrams contributing to Σ_{imp} – and therefore $\Sigma(\mathrm{i}\omega_n, \boldsymbol{k})$ – are taken into account; what is ignored is just their spatial independent parts.

For Hubbard model, the interaction term in the impurity problem is exactly $Un_\uparrow n_\downarrow$, because it is strictly local and is not corrected when electrons on other sites are integrated out. For models with nearest-neighbor interaction, this is no longer correct, because now integrating out other electron modes means screening of the interaction. An even more important fact about models with repulsion between electrons from different sites is the interaction term cannot appear in a single-site model. To solve the above problems, a possible way is to use a Hubbard-Stratonovich transformation and use an auxiliary boson field to introduce the interaction. The resulting single-site model is in an itinerant electron bath and a bosonic bath [5].

3 Going beyond DMFT

Unfortunately, in some scenarios the original single-site DMFT is bound to fail. This is exemplified in phrase transition, in which long-wavelength behaviors are highly important, and a strictly local Σ cannot be the case. A possible direction of improvement is to use an impurity dual Hamiltonian involving a larger cluster of states [6, 7]. The main problem of this approach is the speed: the impurity model concerning a large impurity cluster has to be solved with high accuracy, and this is demanding for existing solvers [8, 9].

Improvement can also be made by relaxing the strict locality condition for the self-energy, which leads to the dynamic vertex approximation. In the dynamic vertex approximation (DΓA), we assume that Σ is not local, but the 2-particle vertex Γ is local. The spatial-varying self-energy can then be calculated from Γ (Fig. 1).

4 DMFT in *ab initio* calculation

As is mentioned above, DMFT (and even its improved versions) assumes strong locality conditions to the system, and therefore has inherent difficulties to capture itinerant behaviors. Common *ab initio* band structure calculation approaches, including DFT and GW, on the other hand, do not capture localized behaviors. Mixing DFT or GW with DMFT is therefore needed for large-scale *ab initio* simulation of materials involving electron localization, or in other words, magnetism.

All electronic structure calculation approaches that use the quasiparticle picture can be summarized as an instance of the minimization problem of the functional

$$\Omega[\mathbf{G}] = \Phi[\mathbf{G}] + \mathrm{Tr}\ln(-\mathbf{G}) - \mathrm{Tr}\left(\left(\mathbf{G}_0^{-1} - \mathbf{G}^{-1}\right)\mathbf{G}\right) \tag{11}$$

with respect to the matrix form of the renormalized Green function G, where Ω is the grand potential and equals to $E - \mu N$ at $T = 0$, and the Luttinger-Ward functional Φ is the sum of of all closed, irreducible, and renormalized skeleton diagrams, and we have

$$\mathbf{\Sigma} = \frac{\delta\Omega}{\delta\mathbf{G}}, \tag{12}$$

so Φ and Ω are some kinds of generating functionals [11, 12].

Specifically, Kohn-Sham density functional theory (DFT) can be formulated in the framework of Luttinger-Ward functional: the Kohn-Sham orbitals are "wave functions" appearing

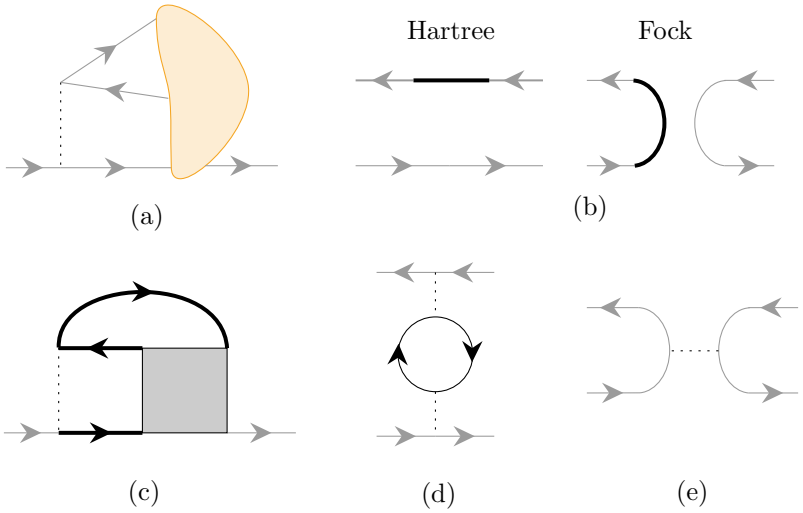

Figure 1: Finding the self-energy from the reducible vertex function [10]. A diagram in the self-energy always starts with a Coulomb interaction vertex, so all self-energy diagrams can be seen as a Coulomb vertex plus a four-leg diagram (a). Here grey lines are external lines, which do not contribute propagator factors and merely provides a momentum value when the diagram is evaluated; bold lines are lines with interaction correction, like self-energy correction for electron lines. When the four-leg diagram is disconnected, we only have two diagrams that are logically possible, and we can find they are just the Hartree diagram and the Fock diagram, and the propagators inside are modified by self-energy correction (b). When there is at least one Coulomb interaction line connecting the upper lines and the lower lines of the four-leg diagram, the four legs have to be linked to four self-energy-corrected electron lines, or otherwise the diagram is not well-formed. Thus we find the sum of all diagrams besides diagrams in (b) is proportion to the reducible two-particle vertex diagram (c), and (a) = (b) + (c) [10]. Specifically, inserting (d) and (e) into the grey box in (c), we get a term in the screening correction (i.e. correction of the interaction line, or "vacuum polarization" in terms of particle physics) and a term in the vertex correction.

in the spectral representation of the one-particle Green function, and the exchange-correlation functional is Φ in terms of the electron number density. In principle, this means the exchange-correlation functional used in DFT can be improved systematically using Feynman diagrammatic techniques [13, 14], although the infamous semiconductor band gap problem persists even with an accurate functional (and actually becomes worse because now there is no cancellation of errors), because we still need to consider the contribution of energy functional discontinuity [14].

On the other hand, the DMFT version of Φ is

$$\Phi = \sum \Phi[G_{\text{imp}}], \tag{13}$$

which is exact when G is indeed completely localized. Therefore to mix DMFT with DFT, we need to replace the part in Φ_{DFT} that could be better described by DMFT, and the resulting Luttinger-Ward functional is

$$\Phi[G] = \Phi_{\text{DFT}}[G] + \Phi_{\text{DMFT}}[G] - \Phi_{\text{DC}}[G], \tag{14}$$

where DC means double-counting [15].

5 Conclusion and discussion

The point of DMFT is to fully utilize the locality in strongly-correlated magnetic systems, and hence map an intractable problem into a hard yet tractable impurity problem.

References

[1] O. Gunnarsson et al. "Breakdown of Traditional Many-Body Theories for Correlated Electrons". In: *Phys. Rev. Lett.* 119 (5 Aug. 2017), p. 056402. DOI: 10.1103/PhysRevLett.119.056402. URL: https://link.aps.org/doi/10.1103/PhysRevLett.119.056402.

[2] Evgeny Kozik, Michel Ferrero, and Antoine Georges. "Nonexistence of the Luttinger-Ward Functional and Misleading Convergence of Skeleton Diagrammatic Series for Hubbard-Like Models". In: *Phys. Rev. Lett.* 114 (15 2015), p. 156402.

[3] Antoine Georges et al. "Dynamical mean-field theory of strongly correlated fermion systems and the limit of infinite dimensions". In: *Reviews of Modern Physics* 68.1 (1996), p. 13.

[4] Antoine Georges and Gabriel Kotliar. "Hubbard model in infinite dimensions". In: *Phys. Rev. B* 45 (12 Mar. 1992), pp. 6479–6483. DOI: 10.1103/PhysRevB.45.6479. URL: https://link.aps.org/doi/10.1103/PhysRevB.45.6479.

[5] Ping Sun and Gabriel Kotliar. "Extended dynamical mean-field theory and *GW* method". In: *Phys. Rev. B* 66.8 (Aug. 2002), p. 085120. DOI: 10.1103/PhysRevB.66.085120. URL: https://link.aps.org/doi/10.1103/PhysRevB.66.085120.

[6] Gabriel Kotliar et al. "Cellular dynamical mean field approach to strongly correlated systems". In: *Physical review letters* 87.18 (2001), p. 186401.

[7] Hyowon Park, Kristjan Haule, and Gabriel Kotliar. "Cluster dynamical mean field theory of the Mott transition". In: *Physical review letters* 101.18 (2008), p. 186403.

[8] Michael Potthoff. "Cluster Extensions of Dynamical Mean-Field Theory". In: *DMFT: From Infinite Dimensions to Real Materials*. 2018, p. 20. URL: https://www.cond-mat.de/events/correl18/manuscripts/potthoff.pdf.

[9] Emanuel Gull et al. "Continuous-time Monte Carlo methods for quantum impurity models". In: *Rev. Mod. Phys.* 83.2 (May 2011). Publisher: American Physical Society, pp. 349–404. DOI: 10.1103/RevModPhys.83.349. URL: https://link.aps.org/doi/10.1103/RevModPhys.83.349.

[10] NE Bickers and SR White. "Conserving approximations for strongly fluctuating electron systems. II. Numerical results and parquet extension". In: *Physical Review B* 43.10 (1991), p. 8044.

[11] J. M. Luttinger and J. C. Ward. "Ground-State Energy of a Many-Fermion System. II". In: *Phys. Rev.* 118 (5 June 1960), pp. 1417–1427. DOI: 10.1103/PhysRev.118.1417. URL: https://link.aps.org/doi/10.1103/PhysRev.118.1417.

[12] Michael Potthoff. "Self-energy-functional approach to systems of correlated electrons". In: *The European Physical Journal B-Condensed Matter and Complex Systems* 32.4 (2003), pp. 429–436.

[13] Ferdi Aryasetiawan, T Miyake, and K Terakura. "Total energy method from many-body formulation". In: *Physical review letters* 88.16 (2002), p. 166401.

[14] Myrta Grüning, Andrea Marini, and Angel Rubio. "Density functionals from many-body perturbation theory: The band gap for semiconductors and insulators". In: *The Journal of chemical physics* 124.15 (2006), p. 154108.

[15] Kristjan Haule and Turan Birol. "Free energy from stationary implementation of the DFT+ DMFT functional". In: *Physical review letters* 115.25 (2015), p. 256402.